SUPPLEMENTARY MATERIAL

MANUSCRIPT TITLE: Molecular insight into the specific interactions of the SARS-CoV-2 Nucleocapsid with RNA and host protein.

6 FIGURES

AUTHORS: Eunjeong Lee, Jasmina S. Redzic, Anthony J. Saviola, Xueni Li, Christopher C. Ebmeier,Tatiana Kutateladze, Kirk Charles Hansen, Rui Zhao, Natalie Ahn, Nikolai N. Sluchanko, Elan Eisenmesser,

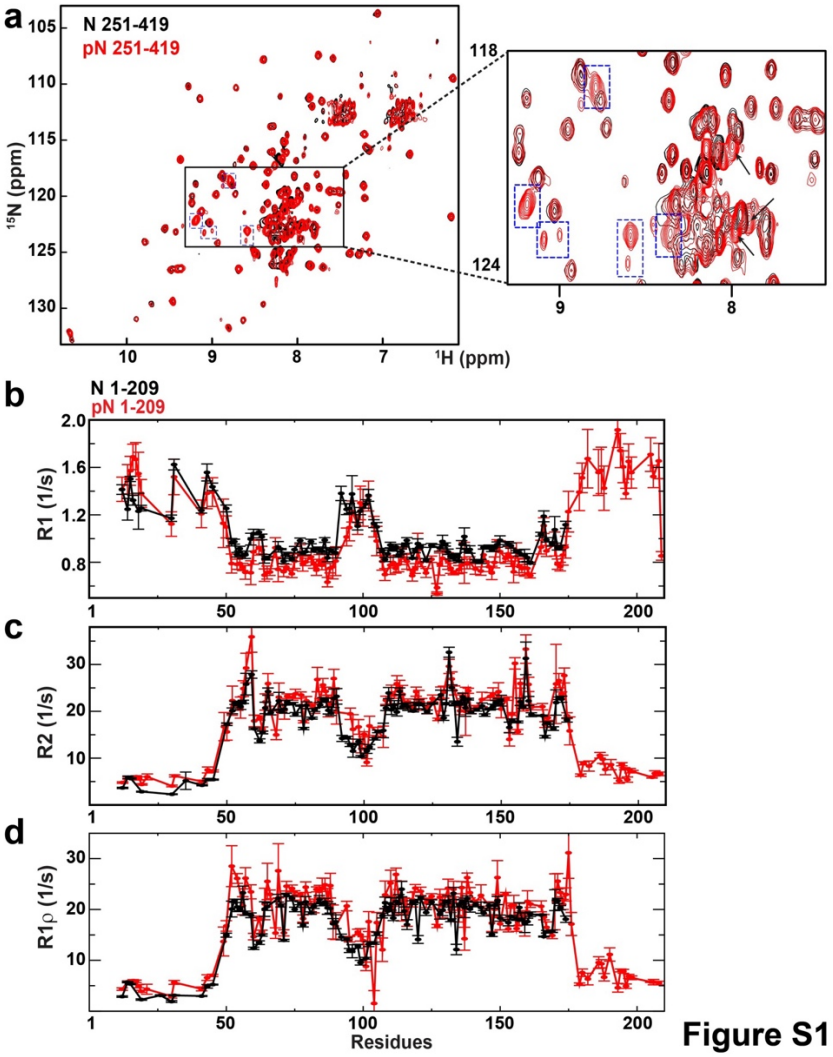

Figure S1

Supplemental Figure 1. Phosphorylation-dependent changes to the N protein.

a) ^{15}N-HSQC spectra of ^{15}N-labeled N 251-419 (black) and phosphorylated N 251-419 (red). Inset highlights resonances that emerge only after phosphorylation.

b) R1 relaxation rates are shown for unphosphorylated N 1-209 (black) and phosphorylated N 1-209 (red).

c) R2 relaxation rates are shown for unphosphorylated N 1-209 (black) and phosphorylated N 1-209 (red).

d) R1ρ relaxation rates are shown for unphosphorylated N 1-209 (black) and phosphorylated N 1-209 (red).

All data were collected at 900 MHz at 35ºC.

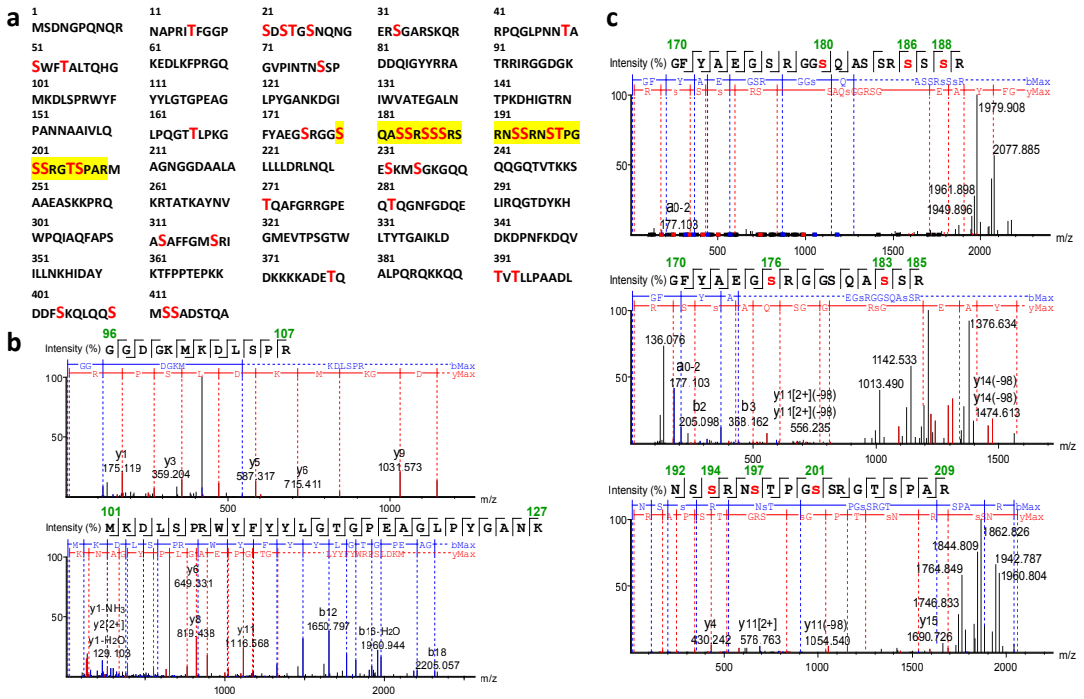

Figure S2

Supplementary Figure 2. N protein phosphorylation sites identified via mass spectrometric analysis with recombinant co-expression of PKA.

a) The position of phosphorylated amino acids in N 1-419 protein are highlighted in red and bold lettesr. Sequence coverage includes 93.3% of the 419 amino acids and 14 out of 15 phosphorylated Ser/Thr within the SR region.

b) LC-MS/MS analysis of the β-hairpin region of the NTD.

c) LC-MS/MS analysis of the SR region that is positioned between the NTD and CTD. The assigned b and y ions which are from fragmentation of each peptide are labeled in blue and red, respectively. Phosphorylated residues are highlighted in red within the peptide sequence.

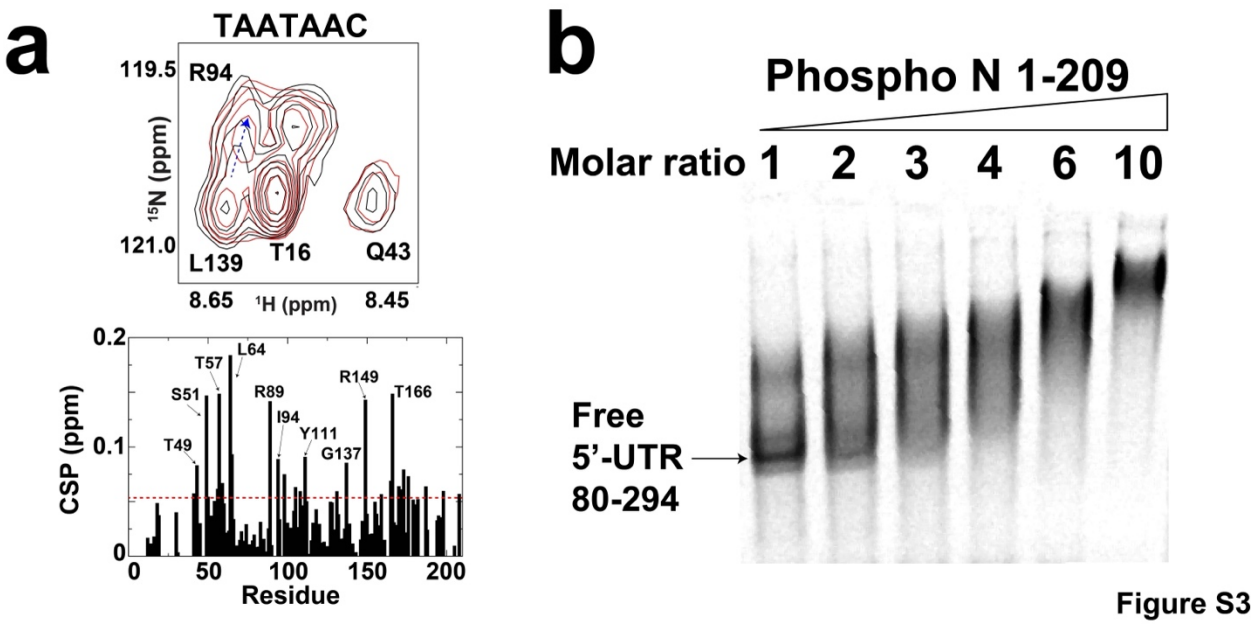

Supplementary Figure 3. DNA binding and vRNP formation with phosphorylated N protein constructs.

a) Overlay of ^{15}N-HSQCs for unphosphorylated N 1-209 (black) and phosphorylated N 1-209 (red) and corresponding CSPs for the entire construct are shown collected at 900 MHz at 35^{o}C.

b) EMSA of phosphorylated N 1-209 and the 5'-UTR 80-294 RNA with increasing concentrations of the latter.

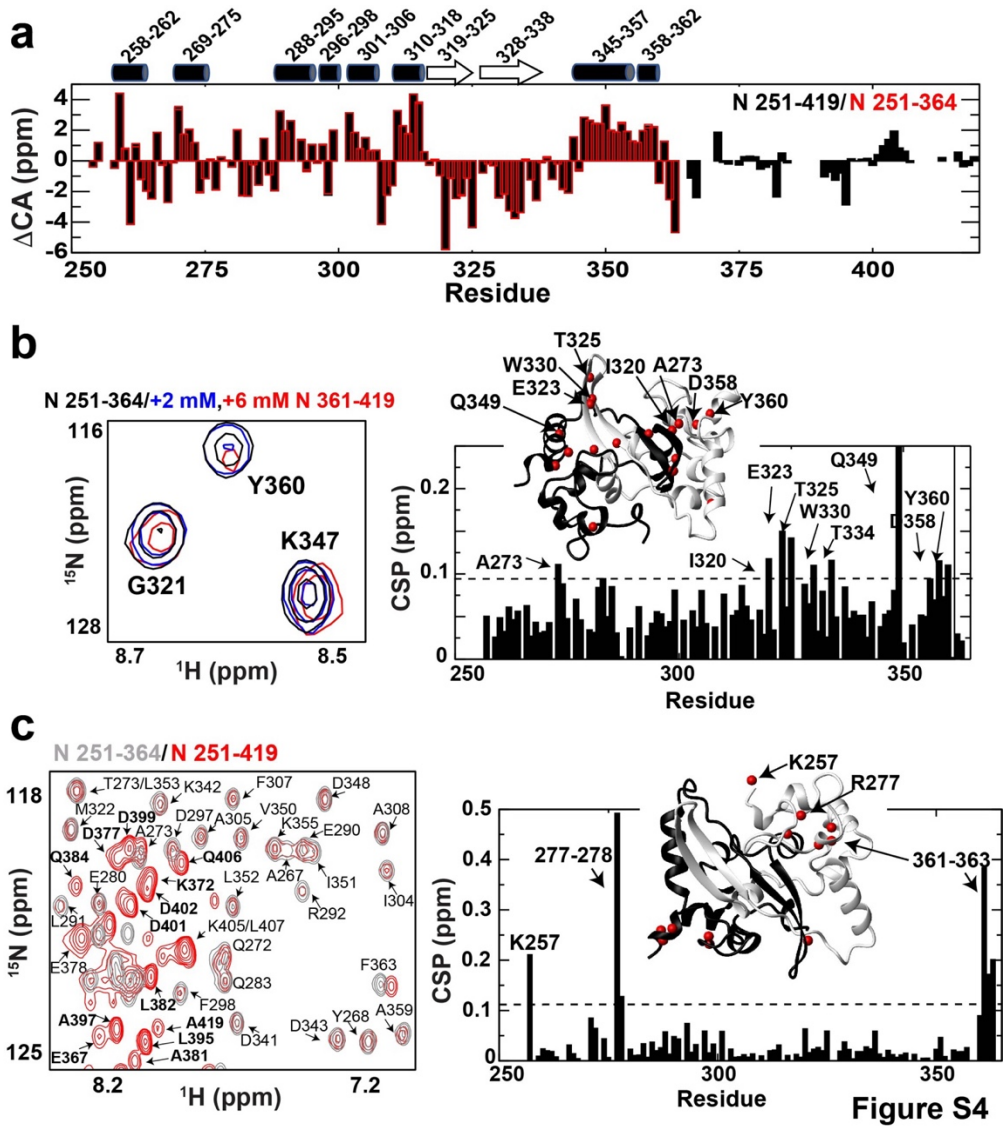

Figure S4

Supplementary Figure 4. Assignments of the C-terminal region of the N protein and probing potential interactions between the disordered CTE (N 365-419) and folded CTD (N 251-364).

a) CA deviations from their random coil resonances (ΔCA) deviations are shown for both N 251-419 (black, closed) and N 251-364 (red, open bar). Secondary structure elements from the X-ray crystal structure of N 251-364 are also shown for comparison.

b) Left: A representative portion of the ^{15}N-HSQC comparison of 500 μM N 251-364 alone (red), in the presence of 2 mM N 361-419 (blue), and in the presence of 6 mM N 361-419 (red). CSPs of N 251-364 upon addition of 6 mM of N 361-419 (right) with the dashed line (0.10 ppm) delineates the sum of the average CSP (0.06 ppm) plus one standard deviation (0.04 ppm). Amides that have larger CSPs than the average plus one standard deviation are mapped onto the X-ray crystal structure of the CTD with flanking regions (red spheres).

c) Left: ^{15}N-HSQC comparison of N 251-364 (gray) and N 251-419 (red). Right: CSPs between N 251-364 and 251-419 with the dashed line (0.11 ppm) delineates the sum of the average CSP (0.04 ppm) plus one standard deviation (0.07 ppm). Residues that have larger CSPs than the average plus one standard deviation are mapped onto the X-ray crystal structure of the C-terminal folded domain (red spheres).

All data were collected at 900 MHz at 35°C.

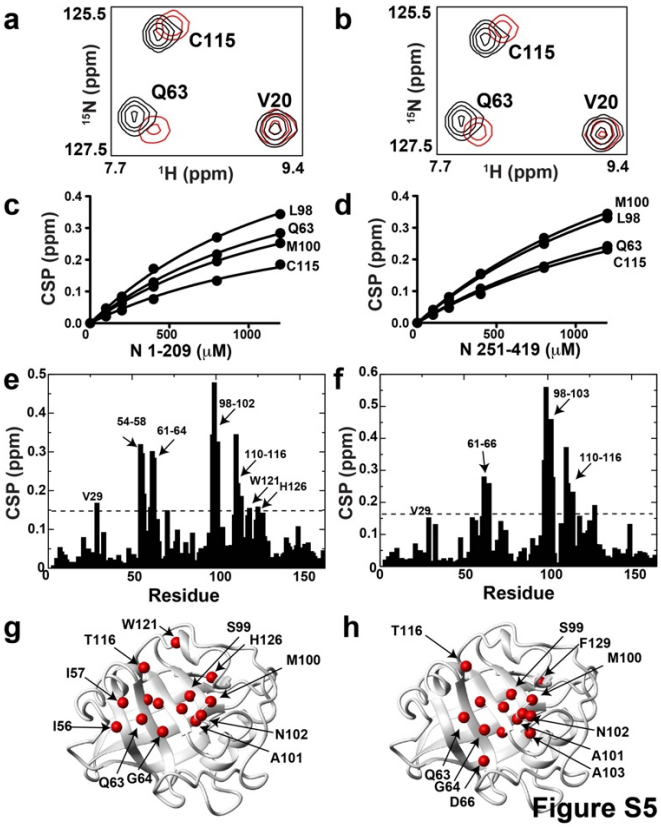

Figure S5

Supplementary Figure 5. Identifying weak N protein interaction sites within CypA.

a) Representative section of the ^{15}N-HSQC spectrum is shown for 500 μM ^{15}N-CypA alone (black) and in the presence of 1.2 mM N 1-209 (red).

b) Representative section of the ^{15}N-HSQC spectrum is shown for 500 μM ^{15}N-CypA alone (black) and in the presence of 1.2 mM N 251-419 (red).

c) Binding isotherm derived from ^{15}N-CypA with the addition of N 1-209 results in a dissociation constant of 0.9 ± 0.1 mM.

d) Binding isotherm derived from ^{15}N-CypA with the addition of N 251-419 results in a dissociation constant of 1.1 ± 0.1 mM.

e) CSPs between ^{15}N-CypA alone and in the presence of 1.2 mM N 1-209 with the dashed line (0.15 ppm) delineating the sum of the average CSP (0.07 ppm) plus one standard deviation (0.08 ppm).

f) CSPs between ^{15}N-CypA alone and in the presence of 1.2 mM N 251-419 with the dashed line (0.16 ppm) delineating the sum of the average CSP (0.07 ppm) plus one standard deviation (0.09 ppm).

g) CSPs greater than the average plus one standard deviation are shown for the addition of N 1-209 (red spheres).

h) CSPs greater than the average plus one standard deviation are shown for the addition of N 251-419 (red spheres).

All experiments probing ^{15}N-labeled CypA were conducted at 900 MHz at 25 °C.

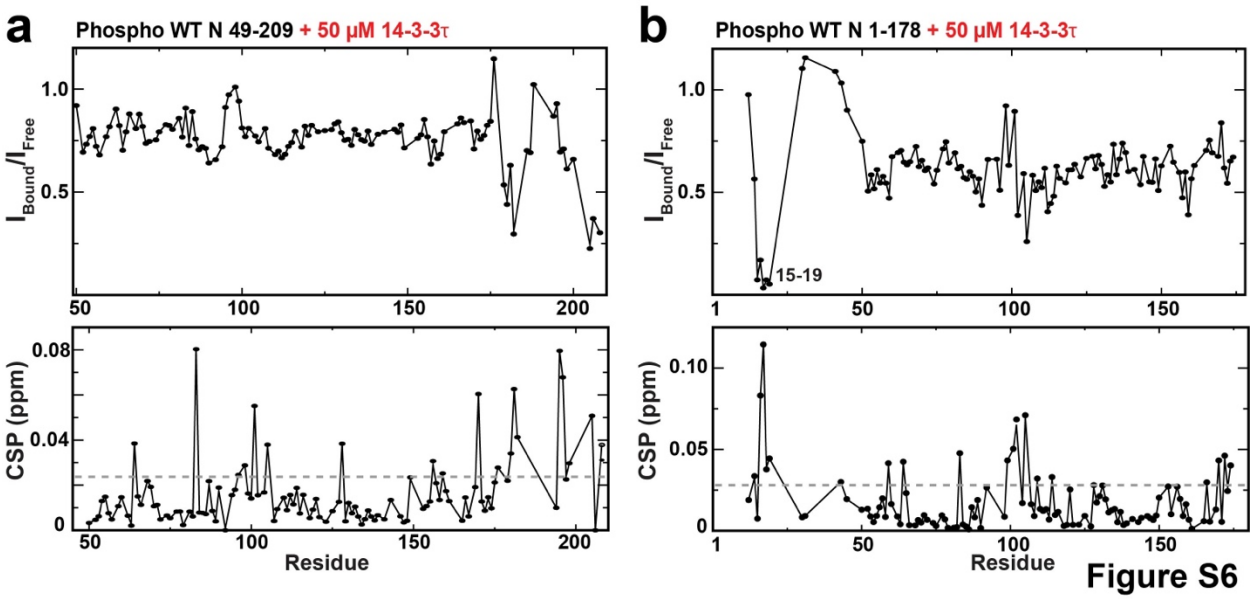

Figure S6

Supplementary Figure 6. Identifying 14-3-3τ interaction sites within the N protein N 49-209 and N 1-178.

a) Top: Per residue intensity of 200 μM phosphorylated N 49-209 in the presence of 50 μM 14-3-3τ over the intensity of N 1-209 alone. Bottom: CSPs between the same samples with gray dashed line delineating the average plus 0.5 standard deviation (0.024 ppm).

b) Top: Per residue intensity of 200 μM phosphorylated N 1-178 in the presence of 50 μM 14-3-3τ over the intensity of N 1-178 alone. Bottom: CSPs between the same samples with gray dashed line delineating the average plus 0.5 standard deviation (0.028 ppm).

All data were collected at 900 MHz at 35°C